# EXTRA STRAIN RATES IN SPILLING BREAKING WAVES

S. K. MISRA[1], J. T. KIRBY[1], M. BROCCHINI[2], M. THOMAS[1], F. VERON[1] AND C. KAMBHAMETTU[1]

*1. University of Delaware,*
*Newark, DE 19716, USA*
*E-mail: shubhra@coastal.udel.edu*

*2. DIAM,*
*Universita' di Genova, Via Montallegro 1,*
*16145 Genova, Italy*

This paper explores the effect of extra strain rates on the turbulence structure of quasi-steady spilling breaking waves. A theoretical model for the single phase turbulent thin layer is developed and the importance of various strain rate terms are analyzed using a perturbation of the governing equations in terms of kinematic and geometric parameters. We find that the effect of extra strain rates is felt at a higher order than the mean simple shear. The theoretical prediction is compared to experimental data obtained from a Particle Image Velocimetry study of a turbulent hydraulic jump. In the breaker mixing layer, the Reynolds shear stress and turbulent kinetic energy distributions don't follow the mean simple shear distribution; instead, they show a correlation with the extra strain induced by streamline curvature.

## 1. Introduction

The motivation for the present study is the need to understand and model free surface turbulence of breaking waves, including its generation, evolution and the effects on the free surface and the bulk of the (irrotational) fluid underneath. Particularly, we focus here on investigating the effect of extra strain rates on the turbulence structure in the curved thin breaker mixing layer. Even though extra strain rate effects seem negligible from a theoretical point of view, previous experiments (Holloway and Tavoularis, 1992) and modeling investigations (Holloway and Tavoularis, 1998) on sheared turbulence have underlined the importance of streamline curvature on the integral scales, anisotropy and spectra of turbulence. Owing to the complexity of the two-phase turbulence in a breaker, theoretical models of spilling breakers have typically relied on simplifying assumptions related to the

bulk characteristics of the flow. The flow is either modeled as a mixing layer (Peregrine and Svendsen, 1978) or in analogy with a hydraulic jump (Madsen and Svendsen, 1983 and Cointe and Tulin, 1994). The details of the turbulence structure are unfortunately lost in such bulk formulations. There have also been numerous experimental studies (Battjes and Sakai, 1981 and Govender *et al*, 2002) on quasi-steady spilling breakers. The breakers were, however, dominated by surface tension and detailed information about the velocity field was limited to the incipient stages of wave breaking (Duncan, 1981, Qiao and Duncan, 2001). It has been deduced experimentally that the local flow beneath the surface and above the shear layer for a quasi-steady spilling breaker can be modeled as a hydraulic jump (Dabiri and Gharib, 1997). In the following section, we reiterate the importance of extra strain rates in modeling the turbulent structure in thin shear layers. In Section 3, we describe the model for the flow in the turbulent thin layer for a quasi-steady spilling breaker, focusing on the Reynolds shear stress and turbulent kinetic energy (TKE) formulations followed by comparisons with data obtained from a Particle Image Velocimetry (PIV) experiment of a turbulent hydraulic jump.

## 2. Extra Strain Rates

Nearly all complex turbulent flows have simple shear layers perturbed by other shear layers, body forces or extra rates of strain ($e$). These can typically be classified as those arising from longitudinal acceleration ($\frac{-\partial U}{\partial \xi}, \frac{\partial V}{\partial \zeta}$), bulk compression or dilation ($\nabla \cdot \mathbf{U}$), rotation of the flow system ($\Omega$) and streamline curvature ($\frac{\partial V}{\partial \xi}$), where $\mathbf{U} = (U, V)$ is the mean velocity in the $(\xi, \zeta)$ coordinate system and $\nabla$ is the two-dimensional gradient operator. Bradshaw, (1973), shows that in fairly thin shear layers typically found in curved free jets and mixing layers, where the simple mean shear is an order of magnitude larger than the extra strain rate ($\frac{\partial U}{\partial \zeta} > 10e$), streamline curvature, caused by surface curvature or helical streamlines, is the most common and probably the most important. The turbulent eddy structure gets modified, which, in turn, influences the higher order Reynolds structure. This essentially means that the effect of streamline curvature is an order of magnitude higher than that predicted by the exact governing equations. This conclusion seems to be valid for all turbulence models, from the simplest local equilibrium formulae for eddy viscosity (Gibson and Rodi, 1981) to the most advanced transport models (Rumsey *et al*, 1999). It is therefore important to consider and account for these extra strain rates since

they not only produce quantitative changes in mixing but also qualitative changes such as instabilities of the mean flow and the virtual elimination of turbulence. For a detailed analysis of streamline curvature effects, see Bradshaw (1973).

## 3. A Model for the turbulent thin layer

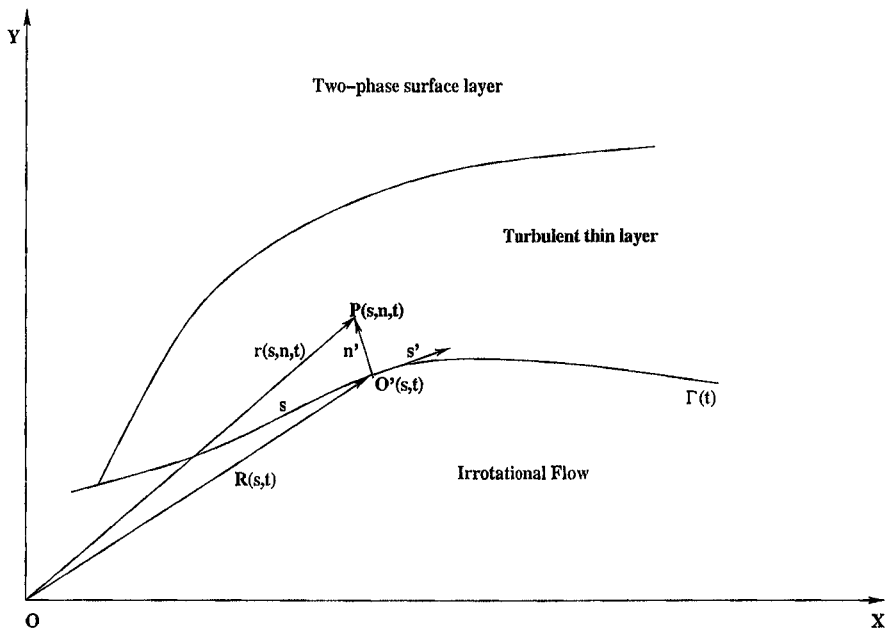


Figure 1. Geometry for the turbulent thin layer (Taken from Brocchini et al, 2004)

Brocchini *et al*, (2004) have been developing a three layer model for the free surface induced turbulence in quasi-steady breaking waves. A schematic picture of the coordinate system is shown in Figure 1. A mobile curvilinear coordinate system $(s, n)$ is used. The top layer is modeled as a two-phase surface layer (Brocchini and Peregrine, 2002) and the governing equations are integrated across the layer to yield boundary conditions for the flow in the single phase turbulent layer. In the single phase thin layer, the equations for conservation of mass and linear momentum are derived including effects of unsteadiness, rotation, curvature and non-hydrostatic

effects. Turbulent averaging is done which leads to Reynolds type equations. A simple $k-\epsilon$ closure for the Reynolds stresses based on Boussinesq eddy viscosity is used. Non-equilibrium for the TKE is allowed by modeling the transport equation for $k$. The governing equations are then recast in dimensionless form in terms of two scaling parameters to characterize the relative importance of the underlying physical mechanisms. The geometric parameter is defined as $\epsilon = \frac{b}{L}$, where $b$ is the layer thickness and $L$ is the length of the region of the wave with the highest curvature. The kinematic parameter $\mu = \frac{\tilde{u}}{U}$ is the ratio of the turbulent velocity scale and the mean stream-wise velocity scale.

The non-dimensional Reynolds shear stress equation is given by

$$- < uv > +\epsilon\kappa n < uv >= \frac{\nu_t}{\mu}\frac{\partial U}{\partial n} + \epsilon\frac{\nu_t}{\mu}\left[U - n\frac{\partial U}{\partial n}\right] + \epsilon^2\frac{\nu_t}{\mu}\frac{\partial V}{\partial s} \quad (1)$$

where $\nu_t$ is the eddy viscosity and $\kappa$ is the geometric curvature. It can be seen that the mean simple shear affects the Reynolds shear stress at leading order whereas the effect of streamline curvature is felt at $O(\epsilon^2)$. This can be seen more clearly by writing the above equation in dimensional form

$$\frac{- < uv >}{\nu_t \frac{\partial U}{\partial n}} = 1 + \alpha_1 \frac{e_1}{\frac{\partial U}{\partial n}} + \alpha_2 \frac{e_2}{\frac{\partial U}{\partial n}} \quad (2)$$

$$\alpha_1 = 1, \qquad e_1 = \frac{\kappa U}{(1-\kappa n)} = \frac{-U}{(n+R)} \quad (3)$$

$$\alpha_2 = 1, \qquad e_1 = \frac{\partial V}{\partial s}\frac{R}{(n+R)} \quad (4)$$

$e_1$ and $e_2$ are the extra strain rates due to geometric curvature and streamline curvature respectively, and are typically much smaller than the simple shear $\frac{\partial U}{\partial n}$. Even though the coefficients $\alpha_1$ and $\alpha_2$ are unity, experimental data from curved shear layers has shown that $\alpha_1$ and $\alpha_2$ are of O(10)!

The production terms in the TKE equation (neglecting rotation effects), including $O(\epsilon)$ terms, can be written as

$$Prod = - < uv > \kappa U - < uv > (1-2\kappa n)\frac{\partial U}{\partial n} - < v^2 > \frac{\partial V}{\partial n} \quad (5)$$
$$+ < u^2 > \left[-\frac{\partial U}{\partial s} + \kappa V\right] + \underbrace{< u^2 > \kappa n \frac{\partial V}{\partial n}}$$

At this order, the Reynolds shear stress thus extracts energy from the mean flow through the simple shear and both the geometric and streamline curvature effects. The longitudinal acceleration strain rates are seen to affect the normal turbulent stresses. Streamline curvature effects are however absent at this order and appear only at $O(\epsilon^2)$. Equation (5) can be compared to the corresponding terms given in Bradshaw (1973)

$$Prod_b = - < uv > \kappa U - < uv > (1 - \kappa n)\frac{\partial U}{\partial n} - < v^2 > \frac{\partial V}{\partial n} \qquad (6)$$
$$+ < u^2 > \left[ -\frac{\partial U}{\partial s} + \kappa V \right] + \underbrace{< v^2 > \kappa n \frac{\partial V}{\partial n}} - < uv > \frac{\partial V}{\partial s}$$

It is to be noted that there is a difference of a factor of two for the second term in the two equations. The under-braced term in equation (5), which is the effect of the longitudinal acceleration and geometric curvature on the normal stress is absent in equation (6). The under-braced term in equation (6), which is the effect of the longitudinal acceleration and geometric curvature on the tangential stress, appears in our equation only at $O(\epsilon^2)$.

## 4. Experiments

The experiment was performed in a recirculating Armfield S6 tilting flume that is 4.8 m long and 30 cm wide, with glass side walls (9 mm thick) and a solid opaque bottom. Water is pumped into the upstream end of the channel through a number of screens and flow straightening devices, after which it flows past an undershot weir. After passing the weir, the super-critical flow transitions to a sub-critical flow by dissipating energy through the formation of a hydraulic jump. Further downstream, the water flows over the downstream gate (which is lowered or raised to fix the location of the jump) and into the reservoir. Further details can be found in Bakunin (1995).

The PIV set-up consisted of a 120 mj/pulse Nd-Yag New Wave solo laser source with a pulse separation of 3 to 5 nanosecs. This was mounted onto a custom-built submersible waterproof periscope which was lowered into the water. The optics were arranged in such a way that the laser beam emerged as a planar light sheet parallel to the flume wall. The laser sheet was aligned with the center plane of the flume away from the side wall boundary layers. The flume bottom and the undershot weir were painted with water resistant black marine paint to minimize reflections from the

laser sheet. The water was seeded with 14 $\mu$m silver coated hollow glass spheres from Potter industries. A Kodak Megaplus 1.0 camera with a 1016 (vertical) $\times$ 1008 (horizontal) pixel CCD array with its image plane parallel to the flume wall, was used to visualize the flow. A Dantec acquisition system was used to acquire the images and store them onto a hard drive. The laser pulses were synchronized with the 30 Hz camera frame rate which ultimately led to a 15 Hz sampling rate for the instantaneous velocity fields. Each experimental run consisted of an ensemble of 1020 image pairs. A robust phase correlation algorithm (Thomas *et al*, 2004) was used to calculate the velocity fields.

## 5. Results

The results are shown for a camera target area of 11.09 cm (horizontal) by 11.18 (vertical). The pixel resolution was 0.011 cm/pixel. The origin of the coordinate system is defined at the flume bottom and at an arbitrary location upstream of the toe. The upstream and downstream depths were $h_0 = 8.625$ and $h_1 = 10.85cm$ respectively. The upstream Froude number calculated from Belanger's equation is $Fr = 1.2$. Even at such a low Froude number, there was breaking and associated air entrainment. The solid line is the ensemble averaged free surface. All the quantities shown are ensemble averaged using a conditional sampling (Antonia, 1981). The top plot of Figure 2 shows the ensemble averaged Reynolds shear stress. The peaks in the Reynolds shear stress and TKE distribution do not coincide with the peaks in the simple shear. There is a definite correlation between the turbulence structure and the stream-wise gradient of the vertical velocity, which is the extra strain rate due to streamline curvature. The magnitudes of $\frac{\partial V}{\partial x}$ are, on an average, an order of magnitude smaller than $\frac{\partial U}{\partial y}$. The increased intensity of both the Reynolds stress and TKE from $\frac{x}{h_0} \sim 0.55$ to $\frac{x}{h_0} \sim 0.75$, is reflected in the increase in the streamline curvature effect. It is interesting to note that the simple shear actually decreases in this region compared to its neighboring values.

## 6. Discussion

The flow in the breaker mixing layer is highly intermittent in both space and time and needs very careful interpretation. The theoretical model predicts that the extra strain rate effects due to geometric and streamline curvature are, respectively, one and two orders of magnitude smaller than

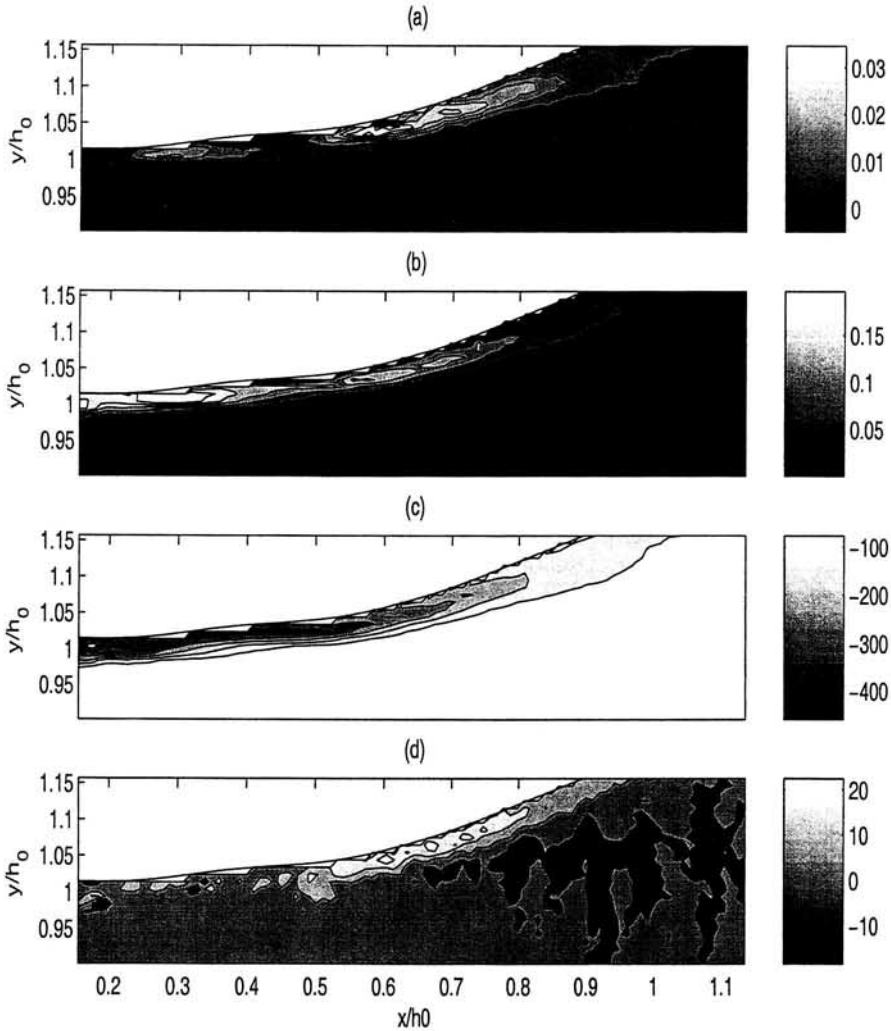


Figure 2. The effect of strain rates on the Reynolds shear stress and TKE. Solid line is the ensemble averaged free surface (a) Reynolds shear stress $(u'v')(m^2/s^2)$ (b) Turbulent kinetic energy $(k)$ $(m^2/s^2)$ (c) Mean simple shear $(\frac{\partial U}{\partial y})$ $(1/s)$ (d) Streamline curvature strain rate $(\frac{\partial V}{\partial x})$ $(1/s)$

the simple shear strain rate. The experimental data on the other hand shows that the peak values in Reynolds shear stress and turbulent kinetic energy distribution are skewed toward the streamline curvature strain rate distribution instead of being correlated with the simple shear. We are currently exploring the effect of free surface and geometric curvature on the turbulence structure and the role played by coherent structures.

## Acknowledgements

We thank Prof. D. H. Peregrine for contributing to the development of the theoretical model and for many useful suggestions. SKM and JTK acknowledge the support of the National Oceanographic Partnership Program.

## References

1. Antonia, R. A. 1981. Conditional sampling in turbulent measurement. *Ann. Rev. Fluid Mech.*, **13**, 131-156
2. Bakunin, J. 1995. Experimental study of hydraulic jumps in low Froude number range, Master's thesis, University of Delaware
3. Battjes, J. A. and Sakai, T. 1981. Velocity field in a steady breaker, *Journal of Fluid Mechanics*, **111**, 421-437
4. Bradshaw, P. 1973. Effects of streamline curvature on turbulent flow, *AGARDograph*, **169**
5. Brocchini, M. and Peregrine, D. H. 2002. The dynamics of strong turbulence at free surfaces. Part 2. The boundary conditions. *Journal of Fluid Mechanics*, **449**, 255-290.
6. Brocchini, M., Misra, S. K., Peregrine, D. H. and Kirby, J. T. 2004. The dynamics of strong turbulence at free surfaces. Part 3 A model for spilling breaking waves. *In Preparation*
7. Cointe, R. and Tulin, M. P. 1994. A theory of steady breakers, *Journal of Fluid Mechanics*, **276**, 1-20
8. Dabiri, D. and Gharib, M. 1997. Experimental investigation of the vorticity generation within a spilling water wave, *Journal of Fluid Mechanics*, **330**, 113-139
9. Duncan, J. H. 1981. An experimental investigation of breaking waves produced by a towed hydrofoil, *Proc. R. Soc. London Ser. A*, **377**, 331-348
10. Gibson, M. M. and Rodi, W. 1981. A Reynolds-stress closure model of turbulence applied to the calculation of a highly curved mixing layer Journal of Fluid Mechanics, **103**, 161-182
11. Govender, K., Alport, M. J., Mocke, G. and Michallet, H. 2002. Video measurements of fluid velocities and water levels in breaking waves, *Physica Scripta*, **T97**, 152-159
12. Holloway, A. G. L. and Tavoularis, S. 1992. The effects of curvature on sheared turbulence, *Journal of Fluid Mechanics*, **237**, 569-603

13. Holloway, A. G. L. and Tavoularis, S. 1998. A geometric explanation of the effects of mild streamline curvature on the integral length scales of sheared turbulence, *Physics of Fluids*, Vol **10**, Number **7**, 1733-1741
14. Madsen, P. A. and Svendsen, I. A. 1983. Turbulent bores and hydraulic jumps, *Journal of Fluid Mechanics*, **129**, 1-25
15. Peregrine, D. H. and Svendsen, I. A. 1978. Spilling breakers, bores and hydraulic jumps, *Proc. 16th Int. Conf. Coastal Engg*, **11**, 540-550
16. Qiao, H. and Duncan, J. H. 2001. Gentle spilling breakers: Crest flow-field evolution, *Journal of Fluid Mechanics*, **439**, 57-85
17. Rumsey, C. L., Gatski, T. B. and Morrison, J. H. 1999. Turbulence Model Predictions of Extra Strain Rate Effects in Strongly-Curved Flows, *AIAA paper*, **99-0157**
18. Thomas, M., Misra, S. K., Kambhamettu, C. and Kirby, J. T. 2004. A robust motion estimation algorithm for PIV, *Measurement Science and Technology*, Under Revision